Check for updates

Intensity directed equalizer for the mitigation of DML chirp induced distortion in dispersion-unmanaged C-band PAM transmission

KUO ZHANG,[1,2] **QUNBI ZHUGE,**[1,2,3,*] **HAIYUN XIN,**[1] **MOHAMED MORSY-OSMAN,**[2] **ESLAM EL-FIKY,**[2] **LILIN YI,**[1] **WEISHENG HU,**[1] AND **DAVID V. PLANT**[2]

[1]*State Key Laboratory of Advanced Optical Communication System and Networks, Department of Electronic Engineering, Shanghai Jiao Tong University, Shanghai, 200240, China*
[2]*Department of Electrical and Computer Engineering, McGill University, Montreal, QC, H3A 2A7, Canada*
[3]*Ciena Corporation, Ottawa, Ontario, K2K 0L1, Canada*
*qunbi.zhuge@mcgill.ca

Abstract: The directly modulated laser (DML) is one of the most cost-effective transmitter options in optical communication systems, but it introduces an additional impairment caused by the interaction between frequency chirp and chromatic dispersion for C-band transmission. In this paper, we propose a low-complexity intensity directed equalizer based on feedforward equalizer and decision feedback equalizer (FFE/DFE) to mitigate the chirp induced distortions, and remarkably improve the transmission performance of PAM signals generated by DML. The equalizer is based on the fact that the directly modulated PAM symbols with different intensity levels have different chirp frequencies, which will lead to different inter-symbol interference (ISI) contributions to their adjacent symbols due to the velocity difference caused by chromatic dispersion. To address this phenomenon, the proposed equalizer employs multiple sets of tap coefficients according to the intensity levels of PAM signals. With this equalizer and a commercial 16.8GHz DML, we demonstrate a 56Gb/s PAM4 transmission over a record 43km SSMF in the C-band without optical dispersion compensation under the 3.8×10^{-3} HD-FEC BER threshold.

References and links

1. IEEE P802.3bs 400 Gb/s Ethernet Task Force, accessed on Dec. 19, 2016. [Online]. Available: *http://www.ieee802.org/3/bs/*
2. Z. Li, I. Shubin, and X. Zhou, "Optical interconnects: recent advances and future challenges," Opt. Express **23**(3), 3717–3720 (2015).
3. X. Liu and F. Effenberger, "Emerging optical access network technologies for 5G wireless," J. Opt. Commun. Netw. **8**(12), B70–B79 (2016).
4. H. Xin, K. Zhang, H. He, W. Hu, and M. Zhang, "Fidelity enhancement in high-data-rate digital mobile fronthaul with sample bits interleaving and unequally-spaced PAM4," Opt. Express **25**(5), 5559–5570 (2017).
5. D. V. Plant, M. Morsy-Osman, and M. Chagnon, "Optical communication systems for datacenter networks." in *Optical Fiber Communications Conference* (OFC) (2017), paper W3B.1.
6. Y. Gao, J. C. Cartledge, S. S.-H. Yam, A. Rezania, and Y. Matsui, "112 Gb/s PAM-4 using a directly modulated laser with linear pre-compensation and nonlinear post-compensation," in *Proceedings of European Conference on Optical Communication* (ECOC) (2016), paper M.2.C.2.
7. Y. Matsui, "28-Gbaud PAM4 and 56-Gb/s NRZ performance comparison using 1310-nm Al-BH DFB lasers," J. Lightwave Technol. **34**(11), 2687 (2016).
8. T. Takahara, T. Tanaka, M. Nishihara, L. Li, Z. Tao, and J. C. Rasmussen, "100-Gb/s (2 x 50-Gb/s) transmission over 80-km using 10-Gb/s class DML," in *Opto-Electron. Commun. Conf.* (OECC) (2012), paper 5A2–2.
9. Z. Li, L. Yi, X. Wang, and W. Hu, "28 Gb/s duobinary signal transmission over 40 km based on 10 GHz DML and PIN for 100 Gb/s PON," Opt. Express **23**(16), 20249–20256 (2015).
10. S. Bae, H. Kim, and Y. Chung, "Transmission of 51.56-Gb/s OOK signal over 15 km of SSMF using directly modulated 1.55-μm DFB laser," in *Optical Fiber Communication Conference* (2016), paper Tu2J.5.

11. N. Eiselt, H. Griesser, J. Wei, A. Dochhan, R. Hohenleitner, M. Ortsiefer, M. Eiselt, C. Neumeyr, J. J. V. Olmos, and I. T. Monroy, "Experimental demonstration of 56 Gbit/s PAM-4 over 15 km and 84 Gbit/s PAM-4 over 1 km SSMF at 1525 nm using a 25G VCSEL," in *Proceedings of European Conference on Optical Communication* (ECOC) (2016), paper Th.1.C.1.
12. M. Kim, S. Bae, H. Kim, and Y. C. Chung, "Transmission of 56-Gb/s PAM-4 signal over 20 km of SSMF using a 1.55-μm directly-modulated laser," in *Optical Fiber Communication Conference* (OFC) (2017), paper Tu2D.6.
13. C. Chen, X. Tang, and Z. Zhang, "Transmission of 56-Gb/s PAM-4 over 26-km single mode fiber using maximum likelihood sequence estimation," in *Optical Fiber Communications Conference* (OFC) (2015), paper Th4A.5.
14. F. Karinou, N. Stojanovic, and C. Prodaniuc, "56 Gb/s 20-km transmission of PAM-4 signal employing an EML in C-band without in-line chromatic dispersion compensation," In *Proceedings of European Conference on Optical Communication* (ECOC) (2016), paper W.4.P1.SC5.50.
15. F. Karinou, N. Stojanovic, C. Prodaniuc, and Q. Zhang, "Experimental demonstration of an electro-absorption modulated laser for high-speed transmissions at 1.55-μm window using digital signal processing," Photonics **4**(1), 9 (2017).
16. J. Zhang, T. Ye, X. Yi, C. Yu, and K. Qiu, "An efficient hybrid equalizer for 50 Gb/s PAM-4 signal transmission over 50 km SSMF in a 10-GHz DML-based IM/DD system," in *Conference on Lasers and Electro-Optics* (CLEO) (2017), paper SF1L.1.
17. J. G. Proakis and D. K. Manolakis, Digital Signal Processing, 4th ed., Pearson, 2006.
18. K. Zhang, Q. Zhuge, H. Xin, M. Morsy-Osman, E. El-Fiky, L. Yi, W. Hu, and D. V. Plant, "Intensity-directed equalizer for chirp compensation enabling DML-based 56Gb/s PAM4 C-band delivery over 35.9km SSMF," in *Proceedings of European Conference on Optical Communication* (ECOC) (2017), paper M.2.F.1.
19. D. Mahgerefteh, Y. Matsui, X. Zheng, and K. McCallion, "Chirp managed laser and applications," IEEE J. Sel. Top. Quantum Electron. **15**(5), 1126–1139 (2010).
20. J. Yu, Z. Jia, M.-F. Huang, M. Haris, P. N. Ji, T. Wang, and G.-K. Chang, "Applications of 40-Gb/s chirp-managed laser in access and metro networks," J. Lightwave Technol. **27**(3), 253–265 (2009).
21. K. Sato, S. Kuwahara, and Y. Miyamoto, "Chirp characteristics of 40-Gb/s directly modulated distributedfeedback laser diodes," J. Lightwave Technol. **23**(11), 3790–3797 (2005).
22. N. Kikuchi, R. Hirai, and T. Fukui, "Non-linearity compensation of highspeed PAM4 signals from directly-modulated laser at high extinction ratio," in *Proceedings of European Conference on Optical Communication* (ECOC) (2016), paper M.2.B.4.
23. N. Stojanovic, Q. Zhang, C. Prodaniuc, and F. Karinou, "Eye deskewing algorithms for PAM modulation formats in IM-DD transmission systems," in *Optical Fiber Communications Conference* (OFC) (2017), paper Tu2D.4.
24. J. M. Castro, R. J. Pimpinella, B. Kose, Y. Huang, A. Novick, and B. Lane, "Eye skew modeling, measurements and mitigation methods for VCSEL PAM-4 channels at data rates over 66 Gb/s," in *Optical Fiber Communications Conference* (OFC) (2017), paper W3G.3.
25. C. C. Wei, "Analysis and iterative equalization of transient and adiabatic chirp effects in DML-based OFDM transmission systems," Opt. Express **20**(23), 25774–25789 (2012).
26. N. Stojanovic, F. Karinou, Z. Qiang, and C. Prodaniuc, "Volterra and Wiener equalizers for short-reach 100G PAM-4 Applications," J. Lightwave Technol. **35**(21), 4583–4594 (2017).

1. Introduction

The continuous growth in the bandwidth demand of internet applications such as high definition TV, online social networks, and cloud computing drives the need for high speed short-haul optical interconnects including datacenter interconnects, mobile fronthaul, metro access, and so forth [1–4]. Compared with long-haul networks, these short-haul networks are very sensitive to cost due to the enormous scale of deployments [5]. Therefore, high speed transceivers at low cost are required in these applications, and intensity modulation and direct detection (IM-DD) has been adopted as the mainstream technology. In IM-DD systems, directly modulated laser (DML)-based transmitters are generally more favorable over externally modulated transmitters based on Mach-Zehnder modulators (MZM) or electro-absorption modulators (EAM). In DML, electrical signals are directly applied to the gain section of the laser cavity, which brings significant benefits such as low cost, high output power and small footprint. Therefore, DMLs have been widely investigated to implement low-cost transmitters [6–12].

However, due to the modulation mechanism of DML, the dependence of frequency chirp on carrier density leads to severe distortions after the directly modulated signal experiences fiber chromatic dispersion. This impairment limits the application of DMLs in C-band transmission, which has advantages such as DWDM compatibility and lower attenuation.

Therefore, most of previous high speed DML-DD based systems are either at the O-band [6,7] or using dispersion compensated fiber (DCF) [8]. For C-band DML-DD transmission without optical dispersion compensation or other optical processing, 56Gb/s 4-level pulse amplitude modulation (PAM4) transmission over 20km fiber was demonstrated in [12], which was achieved by laser parametric optimization and feedforward/decision-feedback equalizer FFE/DFE based digital signal processing (DSP). It is worth mentioning that even using transmitters with external modulators such as MZM [13] and EAM [14,15] and adopting complicated maximum likelihood sequence estimation (MLSE) equalization, the transmission distance of 56Gb/s PAM4 signals was limited within 30km. Here, it should also be pointed out that in a recent work 50km transmission of 50Gb/s (rather than 56Gb/s) signals was realized in a C-band DML-DD system [16]. However, a high-complexity Volterra filter at the receiver side was adopted [17].

In this paper, we propose a novel low-complexity intensity directed equalizer to mitigate the signal distortions caused by the interplay of the DML frequency chirp and chromatic dispersion. A record 43km transmission, to the best of the authors' knowledge, is demonstrated for 56Gb/s PAM4 signals in a C-band DML-DD system without optical dispersion compensation. Based on the fact that PAM4 symbols with different intensity levels induce different interferences to adjacent symbols because of the interaction between adiabatic chirp and chromatic dispersion, the intensity directed FFE/DFE (ID-FFE/ID-DFE) applies four different sets of coefficients to the interfering symbols according to their intensities. Compared with conventional FFE/DFE, the equalizer only adds some simple decision circuits, and thus is of low complexity. This paper is an extension of our previous work in [18]. In addition to more detailed descriptions of the principle and experiment, the following contents are modified or added in this paper: (i) We use a PIN in this paper instead of a PIN-TIA (transimpedance amplifier) in [18], because the PIN has a lower noise and the DML has enough output power to address the reduced sensitivity of PIN. (ii) The complexity of the proposed equalizer is analyzed and compared. (iii) We further propose to apply a conventional FFE before the intensity directed equalizer (pre-FFE + ID-FFE/ID-DFE), which reduces the BER of the 35.9km case from 2.0×10^{-3} to 2.6×10^{-4} (an order of magnitude), and extends the system reach from 35.9km to 43km. (iv) Comparisons between the proposed equalizer and a Volterra filter in terms of complexity and performance are also conducted.

The reminder of the paper is organized as follows. In Section 2, we describe the principle of the proposed intensity directed equalizer. In Section 3, the experimental setup is given. In Section 4, we show the comparison results of the conventional FFE/DFE and the proposed ID-FFE/ID-DFE, and demonstrate the 35.9km transmission with the ID-FFE/ID-DFE. We also illustrate the compensation of chirp-related eye skewing under different distances and different chirp, and study the complexity of the ID-FFE/ID-DFE. In Section 5, we show the results of pre-FFE + ID-FFE/ID-DFE, which enables to reduce the BER of the 35.9km case by an order of magnitude and finally achieves 43km transmission.

2. Principle

The frequency chirp of the DML can be categorized into adiabatic chirp and transient chirp. When a DML is biased far higher than the threshold current, the adiabatic chirp can be more dominant over the transient chirp [19]. Hence, in this work the transient chirp is suppressed by a high output power, and we focus on the adiabatic chirp. Derived from the laser diode rate equations, the adiabatic chirp of a DML can be express as [20]

$$\Delta f = \frac{\alpha}{4\pi} \cdot \kappa \cdot P(t) \tag{1}$$

where $P(t)$ is laser output power, α is laser linewidth enhancement factor, κ is adiabatic chirp coefficient, and both α and κ are positive constants for DMLs. Caused by this adiabatic chirp,

the directly modulated PAM symbols with different intensity levels have different optical frequencies, and thus they travel with different velocities in a dispersive fiber. Therefore, the eye diagram after fiber transmission usually manifests an eye skewing effect, as illustrated in Fig. 1. In addition, other nonlinear distortions are caused. For example, the non-uniform overlap of adjacent symbols will induce edge overshooting and beating noise [21]. For this reason, PAM symbols with different intensity levels have different ISI contributions to their adjacent symbols. However, the conventional FFE/DFE applies one set of coefficients to mitigate ISI, regardless of the symbol intensity levels. As a result, the ISI induced by the eye skewing effect cannot be effectively removed, causing high sensitivity to decision clock jitter, high BER of the least significant bit, and so forth.

Fig. 1. Illustration of the interaction between adiabatic chirp and chromatic dispersion.

A few methods have been proposed to address the skewing effects in PAM4 transmissions [22–24], and in these works the skewing is caused by transceivers instead of the interaction between the DML chirp and CD during transmission. In our work, we propose a novel equalizer based on the conventional FFE/DFE, denoted as intensity directed equalizer, to mitigate the eye skewing effect as well as other nonlinear distortions in DML-based C-band transmission systems. In addition, different from the methods in [22–24], which rely on the estimation or derivation of the time skew, the proposed intensity directed equalizer can adaptively converge to optimal performance for any link conditions.

Note that the proposed equalizer applies to any PAM formats, and we use PAM4 as an example in this work to explain the principle and demonstrate the performance. Different from the conventional FFE/DFE that applies one set of coefficients as shown in Fig. 2(a), the proposed ID-FFE/ID-DFE as depicted in Fig. 2(b) first classifies a symbol into different sets according to its intensity level as shown in the grey inset. Then coefficients from different sets are applied accordingly. Since a PAM4 symbol has four different intensity levels, we apply four sets of coefficients, selected based on three thresholds $\{Th1, Th2, Th3\}$ for ID-FFE and four levels $\{Lv0, Lv1, Lv2, Lv3\}$ for ID-DFE. After classification, the desired tap coefficients from $\{w_{p,0}, w_{p,1}, w_{p,2}, w_{p,3}\}$ and $\{v_{Q,0}, v_{Q,1}, v_{Q,2}, v_{Q,3}\}$ are used for ID-FFE and ID-DFE, respectively. The Fig. 2(b) shows the detailed structure of a $(P + 1)$-tap ID-FFE with K samples per symbol and a Q-tap ID-DFE. From this structure, it is easy to figure out that the $(P + 1)$-tap ID-FFE can be expressed as

$$y_{ID-FFE}(m) = \sum_{i=0}^{P} w_i x(n-i) \tag{2}$$

where $x(\cdot)$ is the originally received signal, $y_{ID-FFE}(\cdot)$ is the signal after ID-FFE, and

$$w_i = \begin{cases} w_{i,0}, & if \ x(n-i) \leq Th1 \\ w_{i,1}, & if \ Th1 < x(n-i) \leq Th2 \\ w_{i,2}, & if \ Th2 < x(n-i) \leq Th3 \\ w_{i,3}, & if \ x(n-i) > Th3 \end{cases} \tag{3}$$

The Q-tap ID-DFE can be expressed as

$$y_{ID-DFE}(m) = y_{ID-FFE}(m) + \sum_{i=1}^{Q} v_i\, y(m-i) \tag{4}$$

Where $y_{ID-DFE}(\cdot)$ and $y(\cdot)$ arethe electrical level sequence before and after the slicing decision circuit as shown in Fig. 2(b), and

$$v_i = \begin{cases} v_{i,0}, & if\ \ y(m-i) = Lv0 \\ v_{i,1}, & if\ \ y(m-i) = Lv1 \\ v_{i,2}, & if\ \ y(m-i) = Lv2 \\ v_{i,3}, & if\ \ y(m-i) = Lv3 \end{cases} \tag{5}$$

We name this scheme as "intensity directed" equalizer, because the difference in the ISI contributions is fundamentally caused by the adiabatic chirp which is determined by optical intensities. For example, the four intensity levels of PAM4 signals lead to four sets of filter coefficients, and the selection of coefficients is directed by the intensity of each PAM4 symbol. As described in Fig. 2(b), the selection of the tap coefficients needs additional decision circuits. However, the complexity of decision for PAM signals is very low since they are single dimensional signals. The switching of the tap coefficients is also very simple to implement in the circuits. Therefore, considering the existing multiplications in the equalizer, the proposed scheme only adds a very low computational complexity to the original FFE/DFE.
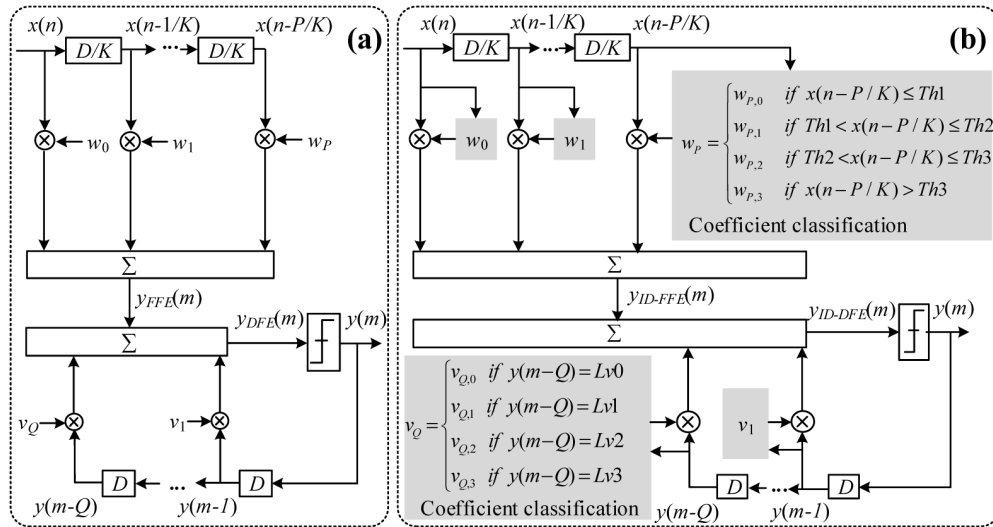
Fig. 2. The detailed structure of (a) conventional (*P*-1)-tap FFE and *Q*-tap DFE, (b) (*P*-1)-tap ID-FFE and *Q*-tap ID-DFE

From Fig. 2, it is clear that, the classification of coefficients is the main modification compared with the conventional equalizer. The accuracy of the decision in the classification plays an important role. In particular, since the equalizer is implemented at the receiver side where signals have suffered from severe impairments from the transmission, the accuracy of the decision in the classification is low, which could influence the effectiveness of the equalization. Consequently, we further propose to implement a conventional FFE at the receiver before the intensity directed equalizer as shown in Fig. 3, namely the pre-FFE + ID-FFE/ID-DFE, in which the pre-FFE here is to improve the decision accuracy of the intensity directed equalizer. In this case, the received signal $x(\cdot)$ is first filtered by a conventional FFE

and then processed by the subsequent ID-FFE/ID-DFE. As will be shown in the following sections, with the assistance of the pre-FFE, the eye skewing problem is shown to be almost completely corrected and the BER is further reduced by an order of magnitude.
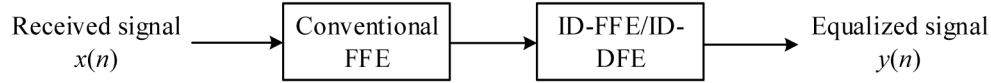

Fig. 3. The block diagram of the pre-FFE + ID-FFE/ID-DFE.

3. Experimental setup

Figure 4 plots the experimental setup. A 6-bit digital-to-analog converter (DAC) (Micram, ~20GHz bandwidth) together with an FPGA board is used to generate PAM4 signals with periodic 2^{14} random bit sequences. The DAC is operated with one sample per symbol at 28GSa/s. No pre-compensation is used here so that the 6-bit DAC can be replaced by a cheaper 2-bit one. After a radio frequency (RF) amplifier (SHF806) and a RF attenuator, the electrical signal is applied to modulate a commercial C-band DML with 16.8GHz 3dB bandwidth and ~13.5dBm saturation power. A >10dBm optical output power is adopted to make the adiabatic chirp more dominant than the transient chirp, and it can also help suppress the potential skewing effect due to signal dependent rise/fall time [22, 24], which means the distortions in the experiment should be mostly caused by the adiabatic chirp. After SSMF transmission, the optical signal is first attenuated by a variable optical attenuator (VOA), and then enters into a PIN without TIA (Finisar, ~50GHz bandwidth). A real-time oscilloscope (RTO) (Keysight) with an 80GSa/s sampling rate is employed to digitize the received signal for offline DSP. The bandwidth of the RTO is internally limited to 28GHz in order to suppress the high frequency noise of the PIN. In the offline DSP, FFE or ID-FFE is operated with 2 samples per symbol and DFE or ID-DFE is operated with 1 sample per symbol. The tap coefficients of all the equalizers are determined by a minimum mean square error estimation. Here, we consider three types of DSP as aforementioned in the Section 2: (i) conventional FFE/DFE as shown in Fig. 2(a); (ii) ID-FFE/ID-DFE as shown in Fig. 2(b); and (iii) pre-FFE + ID-FFE/ID-DFE as shown in Fig. 3.
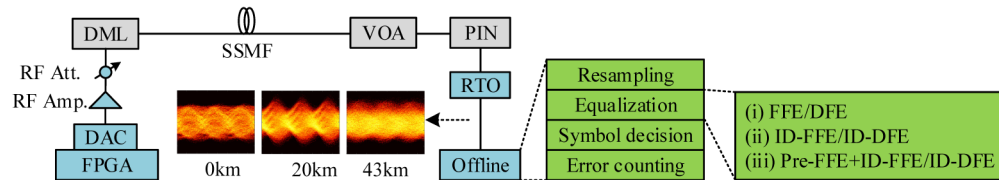

Fig. 4. Experimental setup. FPGA: field-programmable gate array; DAC: digital to analog converter; VOA: variable optical attenuator; RTO: real-time oscilloscope. Eye diagrams after fiber transmission are also shown.

4. Transmission results of ID-FFE/ID-DFE

4.1 Transmission performance

For DML-based systems, the transmission performance is influenced by the output optical power of the DML and the peak-to-peak voltage (Vpp) of the RF signal. A higher output power helps suppress the transient chirp and enhance the device bandwidth, but decreases the extinction ratio (ER). A lower Vpp helps generate a lower adiabatic chirp, but also decreases the ER [19]. Therefore, in the transmission, the output power of the DML and the Vpp of the PAM4 signal are optimized for each transmission distance to achieve a best performance for each case. The output powers are 10, 11, 12.5 and 12.5dBm and the Vpp's are 1.6, 1.0, 1.0 and 0.76V for 0, 20, 30 and 35.9km distances, respectively. As a consequence, the ERs of the output signals are respectively 3.5, 1.7, 1.5 and 1.25dB for 0, 20, 30 and 35.9km distances.

Here it should be noted that we set the ERs of the long-distance cases to be small to suppress the chirp effect. Nevertheless, the decrease of ER in a long distance, e.g. 30~40km, does not significantly degrade the receiver sensitivity because of the frequency modulation (FM) to amplitude modulation (AM) conversion [21] for directly modulated signals in a dispersive fiber. In the offline DSP, we utilize 21-tap half-symbol-spaced [$K = 2$ in Fig. 2] FFE or ID-FFE and 15-tap DFE or ID-DFE. The BER performances under four DSP conditions, including FFE, FFE/DFE, ID-FFE and ID-FFE/ID-DFE, are compared and plotted in Fig. 5 for each distance. The scatter diagrams of FFE/DFE and ID-FFE/ID-DFE when the received power is 5dBm are inserted. Each of the scatter diagrams is comprised of 170,000 electrical-level points of the $y_{ID-DFE}(\cdot)$ in Eq. (4) or the counterpart $y_{DFE}(\cdot)$. Meanwhile, to show the eye skewing effect caused by the interaction between chirp and dispersion, the eye diagrams after FFE and ID-FFE are also provided in Table 1, which is obtained by resampling the originally received signal to 16 samples per symbol and inserting 7 zeros between adjacent half-symbol-spaced taps in the offline processing.
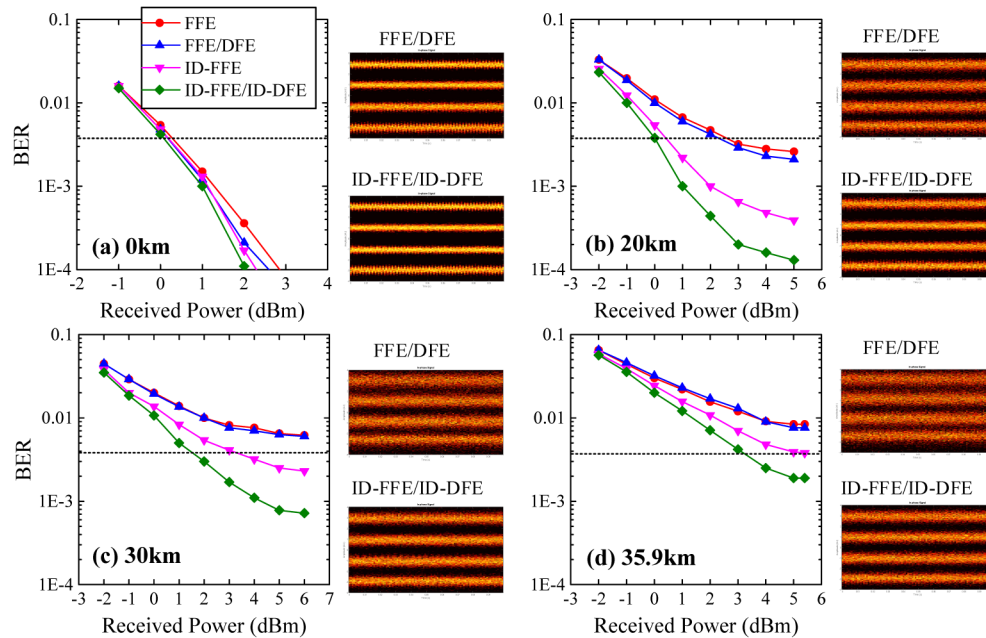
Fig. 5. BER performance with different distances. The inset scatter diagrams are measured with 5dBm received optical power.
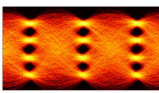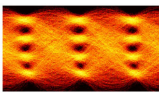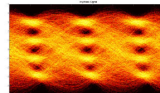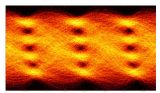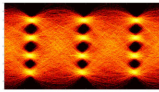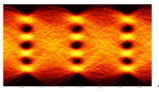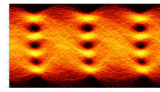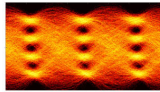
In the back-to-back (BtB) case as shown in Fig. 5(a), the proposed equalizer slightly outperforms the conventional equalizer, which is mainly due to the mitigation of some transceiver distortions. In this case, no BER floor is observed, and both the conventional FFE/DFE and the proposed ID-FFE/ID-DFE work properly to compensate the impairments. Also, as shown in Table 1, the eye skewing effect is not observed with both the conventional FFE and the ID-FFE because the chromatic dispersion is not present in the BtB case.

In the 20km transmission case in Fig. 5(b), significant BER distinctions appear among these four DSPs. When the conventional FFE is adopted, the BER is 2.1×10^{-3}, which is very close to the HD-FEC BER threshold. The DFE only brings a very small improvement. This result is very similar to the previous study reported in [12] where they realized 20km transmission by adopting FFE/DFE and optimizing the laser parameters. In contrast, when the proposed ID-FFE is adopted, the BER decreases dramatically and reaches 3.9×10^{-4}. The skewing effect of the eye diagram in Table 1 is shown to be greatly alleviated compared with

the eye diagram of FFE. Moreover, with the ID-FFE/ID-DFE, the performance is further improved and the BER decreases to 1.3×10^{-4}, which is below the KP4 BER threshold (2×10^{-4}).

In the 30km transmission case, similar performance distinctions among the four DSPs are observed as the 20km case. In this case the BER of the conventional FFE/DFE is 6.0×10^{-3}, which can no longer satisfy the HD-FEC requirement. In contrast, the BER of the proposed ID-FFE/ID-DFE is 7.2×10^{-4}, which outperforms the conventional FFE/DFE by almost an order of magnitude. Finally, in the 35.9km transmission case, a BER of 2.0×10^{-3} is achieved with the ID-FFE/ID-DFE.

Table 1. Eye Skew Suppression and ISI Mitigation with Different Distances

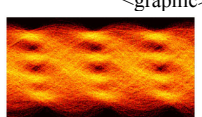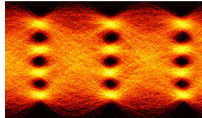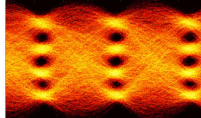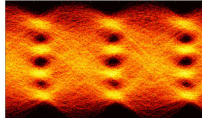|	0km	20km	30km	35.9km
FFE				
ID-FFE				
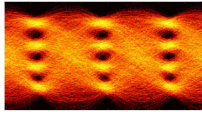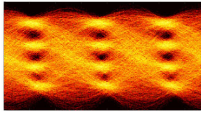
In general, as the transmission distance increases, stronger ISI and more prominent eye skewing effect are observed after the conventional FFE as shown in Table 1. This phenomenon results from the fact that a larger chromatic dispersion in a longer fiber link in combination with the frequency chirp causes a larger velocity difference between different intensity levels of PAM4 signals. In contrast, by adopting the proposed ID-FFE, the skewing effect is clearly alleviated and the ISI distortion is also mitigated, which results in a significant transmission performance improvement compared with the conventional FFE. However, since there is still some residual eye skewing effect after ID-FFE as shown in Table 1, the performance is further improved by using ID-DFE.

4.2 Illustration of eye diagrams with different chirp levels

In Section 4.1, we have shown that a longer transmission distance causes a severer eye skewing effect, and the proposed ID-FFE/ID-DFE can effectively address this problem. In this part we investigate the suppression of the eye skewing effect under different chirp levels. The 20km transmission case is investigated here because it has a relatively better performance and more broadened eye diagrams which give a clearer visual comparison. Since a higher Vpp means a larger laser carrier density difference between different intensity levels and produces a larger adiabatic frequency chirp, we change the chirp level by applying different Vpp. The eye diagrams after FFE and ID-FFE are listed in Table 2. In this table, it is apparent that when the chirp gets larger as Vpp increases, the eye diagram after FFE shows an enhanced skewing effect, which causes a much stronger ISI. This is mainly because that a larger frequency chirp leads to larger velocity difference between intensity levels. On the contrary, when the ID-FFE is adopted, the eye skewing is well removed addressed for all the three cases.

Table 2. Eye Skew Suppression and ISI Mitigation with Different Chirp

	Small chirp (Vpp = 0.9V)	Medium chirp (Vpp = 1.2V)	Large chirp (Vpp = 1.5V)

FE			
D-FFE			

4.3 Tap complexity analysis

The complexity of an equalizer is mainly determined by two factors. The first one is the structure of the equalizer, which is shown to be very simple for the proposed ID-FFE/ID-DFE since only a few simple decision circuits are added compared with the conventional FFE/DFE. The other is the required tap number. In this subsection, we will investigate the required tap number of the ID-FFE/ID-DFE in the 35.9km transmission case and compare it with the conventional equalizer.

We first study the BER performance with different tap numbers. The received optical power is fixed at 5dBm. We change the ID-FFE tap number from 3 to 31 and ID-DFE tap number from 1 to 15. The BER contour diagram is depicted in Fig. 6. Obviously, the BER decreases with the increase of the tap number. It is shown that a 13-tap ID-FFE and a 5-tap ID-DFE will satisfy the 3.8×10^{-3} HD-FEC BER threshold. Therefore, the intensity directed equalizer has a relatively low complexity.
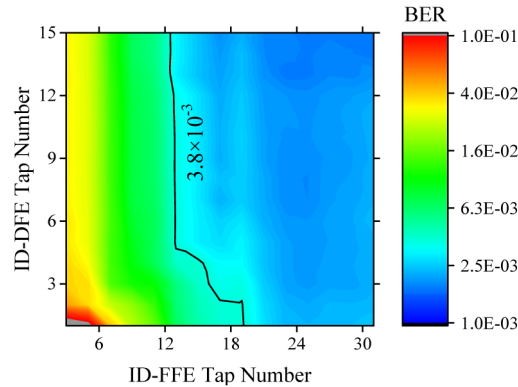

Fig. 6. BER performance with difference tap numbers of ID-FFE and ID-DFE when received power is 5dBm and transmission distance is 35.9km.

Next, the required tap number of the proposed equalizer is compared with the conventional equalizer. Since the conventional DFE has very little improvement to the BER performance, we only compare the FFE and the ID-FFE here. As shown in Fig. 7, with the increase of tap number, the performances of both equalizers are gradually improved. The two BER curves present similar decreasing trends, and both of them reach a floor when the tap number is around 21. This result implies that the proposed ID-FFE does not require additional taps compared with the conventional FFE to achieve the optimal performance.
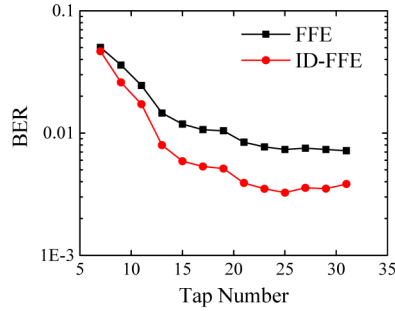
Fig. 7. Comparison of the required tap number of FFE and ID-FFE.

5. Transmission results of the pre-FFE + ID-FFE/ID-DFE

In the proposed ID-FFE/ID-DFE, the intensity level is used to select the tap coefficient as shown in Fig. 2. Therefore, the decision accuracy of the intensity level affects the effectiveness of the equalizer. However, after fiber transmission, the signal is so distorted that the BER before the DSP is on a 10^{-1} level as shown in Fig. 8. Hence, the decision accuracy in the ID-FFE stage is quite low. Therefore, in this section, we propose to apply a conventional FFE before using the ID-FFE/ID-DFE in order to improve the decision accuracy of the ID-FFE stage.

Following the experiments in Section 4, we first conduct the investigations in the 35.9km transmission case. A 21-tap pre-FFE is applied before the ID-FFE/ID-DFE. The BER versus the received optical power is plotted in Fig. 8(a). In this figure, when the received power is 5.4dBm, it is shown that the pre-FFE first reduces the BER from 1.8×10^{-1} to 9×10^{-3}. After that, the subsequent ID-FFE/ID-DFE reaches a BER of 2.6×10^{-4}. Compared with the ID-FFE/ID-DFE only case, of which the BER is 2.0×10^{-3}, the pre-FFE + ID-FFE/ID-DFE improves the performance by almost an order of magnitude. The resulted eye diagrams of ID-FFE with and without pre-FFE is given in Table 3, which clearly illustrates that the pre-FFE is able to completely correct the residual eye skewing effect of the ID-FFE and effectively remove the ISI.

We then measure the transmission performance with longer distances in order to obtain the maximum achievable distance with pre-FFE + ID-FFE/ID-DFE. It is found that, the BER finally reaches the HD-FEC threshold after 43km transmission. In the 43km transmission case, the laser power is 12.5dBm and the Vpp of the electrical signal is set to 0.76V. The performance results are shown in Fig. 8(b). When the received power is 4.8dBm, the pre-FFE first reduces the BER from 2.1×10^{-1} to 4×10^{-2}. Then, the subsequent ID-FFE/ID-DFE reaches a BER of 3.6×10^{-3} below the HD-FEC threshold.
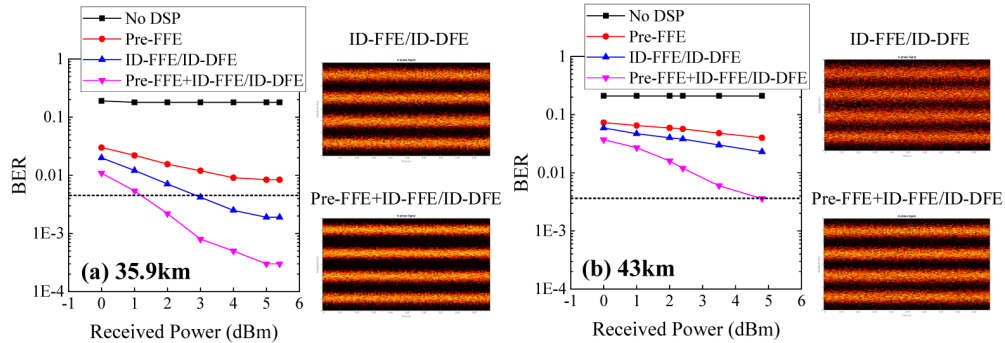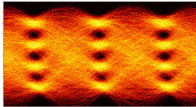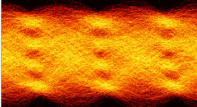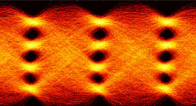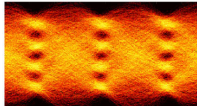

Fig. 8. The BER performance of ID-FFE/ID-DFE w/ and w/o pre-FFE.

Table 3. Eye Diagrams of ID-FFE and pre-FFE + ID-FFE with 35.9km and 43km Distances

	35.9km	43km
ID-FFE	<graphic></graphic>	<graphic></graphic>
Pre-FFE + ID-FFE	<graphic></graphic>	<graphic></graphic>

Next, to investigate the limitation of transmission distance, we measure the fiber frequency response of the 30km, 35.9km and 43km transmission cases as shown in Fig. 9. Since the frequency curve is obtained with the offline data rather than a vector network analyzer, it is not very smooth especially for the high frequency part. However, one can still clearly observe that the first power dip of the frequency curve in the 43km transmission case is located at ~14GHz, which is the Nyquist bandwidth of 56Gb/s PAM4 signals. Therefore, in this case the transmission performance is now dominantly limited by the bandwidth limitation, which is mainly caused by the chromatic dispersion induced power fading. In other words, the chirp-related impairments have been well addressed by the proposed equalizer and is thus not a limiting factor to further increase the distance. Also, it is worth mentioning that the frequency curve presents a rising trend in the low frequency part from 0GHz to ~10GHz, which is mainly caused by the chirp characteristics of DMLs [25], and is a little different from other transmitters such as MZM.
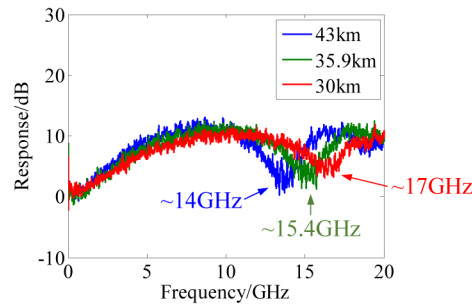

Fig. 9. Frequency responses of the 43, 35.9 and 30km transmission cases

Finally, since the pre-FFE will increase the total DSP complexity, we investigate the required tap number of the pre-FFE in the 43km transmission case. We change the tap number of the pre-FFE from 3 to 31, while fixing the tap number of ID-FFE and ID-DFE at 21 and 15, respectively. The BER performance of the pre-FFE + ID-FFE/ID-DFE is given in Fig. 10. As it illustrates, the BER reaches the HD-FEC threshold when the tap number is 21.
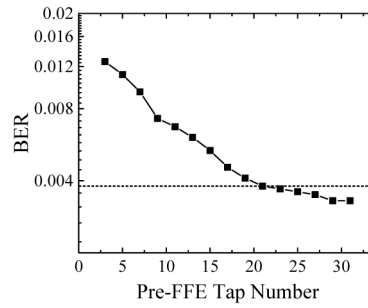
Fig. 10. BER performance versus the tap number of the pre-FFE.

6. Comparison with Volterra filter

It is well known that Volterra filter is a universal equalization scheme that can mitigate all kinds of linear and nonlinear distortions [26]. Thus, to better illustrate the advantages of the proposed equalizer that specifically serves for distortion mitigation in DML-based C-band transmission systems, we conduct the comparison of the performance and complexity between the Volterra filter and the proposed equalizer in this section. In particular, they are compared in three transmission cases: (i) 20km, (ii) 35.9km and (iii) 43km.

The BER performance versus the memory length of the 2nd order kernels are plotted in Fig. 11. Firstly, in the 20km transmission case, it is found that the 3rd order of the Volterra filter leads to no improvement, so we only apply the 1st and 2nd order kernels and the memory length of the 1st order kernels is fixed to 23 taps. We can observe that the Volterra filter outperforms the proposed equalizer when the memory length of the 2nd order kernels is sufficiently large. However, with the same performance the complexity of the Volterra filter is much larger. In particular, to reach the BER of ID-FFE/ID-DFE, the memory length of the Volterra filter should be (23, 11, 0) with 23 1st order kernels and 66 2nd order kernels, which requires in total 155 real multipliers. To reach the BER of pre-FFE + ID-FFE/ID-DFE, the memory length of the Volterra filter should be (23, 13, 0), which is comprised of 205 real multipliers. In these two cases, the tap number of the pre-FFE, ID-FFE and ID-DFE are respectively 21, 21 and 15, so the multiplier number of the ID-FFE/ID-DFE and pre-FFE + ID-FFE/ID-DFE are only 36 and 51.

Secondly, in the 35.9km and 43km cases, the memory length of the 1st order kernels and 3rd order kernels are set to be 31 and 3, respectively, and further increasing the length of 3rd order kernels is verified to obtain no performance improvement. It is shown that the Volterra filter is able to achieve a lower BER than the ID-FFE/ID-DFE, but always a higher BER than the pre-FFE + ID-FFE/ID-DFE. Particularly in the 43km transmission case, the BER of pre-FFE + ID-FFE/ID-DFE can be as low as 3×10^{-3}, whereas the Volterra filter can only reach 1×10^{-2}. Further, the complexity of the Volterra filter can be much higher than the proposed equalizer as discussed earlier. It should be noted that the complexity of the Volterra filter might be significantly reduced using a "truncated" or "sparse" scheme [26], and this investigation is beyond the scope of this paper. Therefore, in these two transmission distances, the pre-FFE + ID-FFE/ID-DFE achieves better performance than the Volterra filter with a potentially lower complexity.

.... BER of ID-FFE/ID-DFE
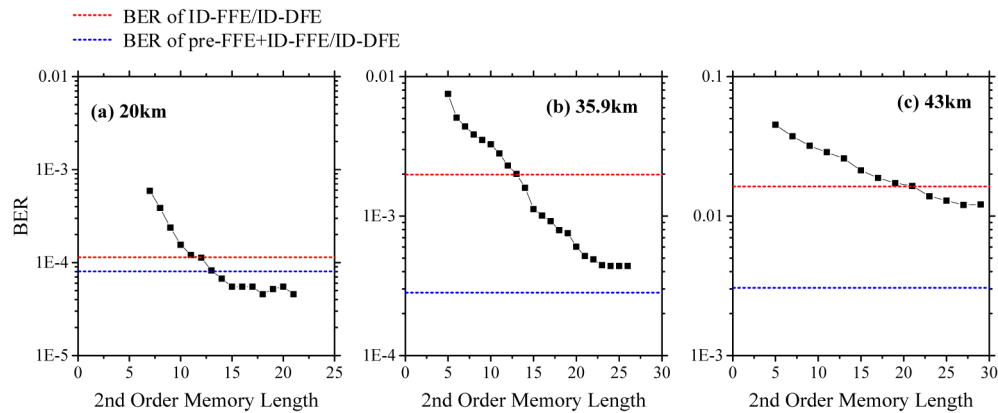....... BER of pre-FFE+ID-FFE/ID-DFE

Fig. 11. BER performances of the 2nd order memory length of Volterra filter. The BER of the ID-FFE/ID-DFE and the pre-FFE + ID-FFE/ID-DFE are also depicted as references.

7. Conclusions

In this paper, we have proposed and experimentally demonstrated a novel intensity directed equalizer which is able to remarkably improve the transmission performance of DML-DD systems. The nonlinear distortions especially the eye skewing effect of PAM signals due to the interaction of DML chirp and fiber chromatic dispersion can be well addressed. Compared with conventional FFE/DFE, the structure of the ID-FFE/ID-DFE only adds a few simple decision circuits and the required tap number of the ID-FFE/ID-DFE is experimentally verified to be almost the same. The transmission results show that the proposed ID-FFE/ID-DFE can extend the transmission distance of 56Gb/s PAM4 signals from 20km to 35.9km compared with the conventional FFE/DFE. By introducing a pre-FFE before the ID-FFE/ID-DFE, we further reduce the BER of the 35.9km case by an order of magnitude and finally realize 43km distance transmission.

Funding